PHYC30170 Physics with Astronomy and Space Science Lab 1; An Investigation into Compton Scattering

Daragh Hollman*
(Dated: March 3, 2023)

I. INTRODUCTION

Compton scattering is the interaction in the collision of a gamma ray with a free electron [1]. In this interaction the gamma ray imparts some of its energy to the electron as it scatters away at an angle. It is important to understand how gamma rays interact with other particles, and Compton scattering is one of the tools which helps to bring about that understanding. Compton scattering has many applications in radiobiology, biomedical science, and in astrophysics [2][3][4] including x-ray imaging and the study of active galactic nuclei.

II. ENERGY AND CROSS-SECTION DETERMINATION

A. Theory

1. Energy Determination

The Compton scattering interaction can be described with the same kinematic equations that describe the collision of two balls in a game of snooker [1]. The interaction is shown in figure 1. An incoming gamma ray (photon) of energy E_γ collides with an electron at rest which results in the gamma being scattered off with reduced energy $E_{\gamma'}$ at some angle θ, imparting kinetic energy to the electron. The electron gains energy E_e and it itself scatters at an angle ϕ.

The energy of the gamma ray after scattering can be calculated using the principles of the conservation of energy and momentum. By the conservation of energy the energy of the incident gamma ray is equal to the energy of the scattered gamma ray and the kinetic energy of the scattered electron, we have:

$$E_\gamma = E_{\gamma'} + E_e \tag{1}$$

Similarly, by the conservation of momentum, the momentum of the incident gamma ray is equal to the momentum of the scattered components. This can be broken up into the components along each axis as follows. In the x direction we have:

$$\frac{hf}{c} = \underbrace{\frac{hf'}{c}\cos\theta}_{\text{scattered gamma ray}} + \underbrace{mv\cos\phi}_{\text{scattered electron}} \tag{2}$$

and in the y direction with zero initial momentum we have:

$$0 = \underbrace{\frac{hf}{c}\sin\theta}_{\text{scattered gamma ray}} - \underbrace{mv\sin\phi}_{\text{scattered electron}} \tag{3}$$

Note that as $E_\gamma = hf$ we also have $E_{\gamma'} = hf'$, and that m represents the relativistic mass of the electron, $m = \gamma m_0$, where here m_0 is the rest mass of the electron and γ represents the Lorentz factor, $\gamma = \left(1 - \frac{v^2}{c^2}\right)^{-1/2}$.

These three equations can be solved to give an equation for the energy of the scattered gamma ray, $E_{\gamma'}$, in terms of the incident gamma ray energy, E_γ, the rest mass energy o the electron, m_0c^2, and the scattering angle, θ [1].

$$E_{\gamma'} = \frac{E_\gamma}{1 + \frac{E_\gamma}{m_0c^2}(1 - \cos\theta)} \tag{4}$$

We know the electron rest mass to be $m_0c^2 = 0.511\,\text{MeV}$ and we know that the gamma rays from the Caesium-137 source used in this experiment have energy $0.662\,\text{MeV}$. As as a result of this, we can represent the energy of the scattered gamma ray in terms of the scattering angle only. We find that:

$$\frac{1}{E_{\gamma'}} = 1.51 + 1.956\,(1 - \cos\theta) \tag{5}$$

and hence it is clear that the inverse of the energy of the scattered ray has a linear relationship with one minus the cosign of the angle it scattered at.

2. Cross-Section Determination

The differential cross-section is the fraction of the total number of scattered particles that emerge from a solid angle [5]. In Compton scattering, the differential cross-section is the probability for each angle that an incident gamma ray is scattered [1]. The Klein-Nishina formula is an equation of the differential cross-section treated quantum mechanically [6]. In a simplified (classical) form we have:

$$\frac{d\sigma}{d\Omega} = \frac{r_0}{2}\left(\frac{1 + \cos^2\theta}{[1 + \alpha(1 - \cos\theta)]^2}\right) \times \left(1 + \frac{\alpha^2(1 - \cos\theta)^2}{(1 + \cos^2\theta)(1 + \alpha[1 - \cos\theta])}\right) \tag{6}$$

* daragh.hollman@ucdconnect.ie

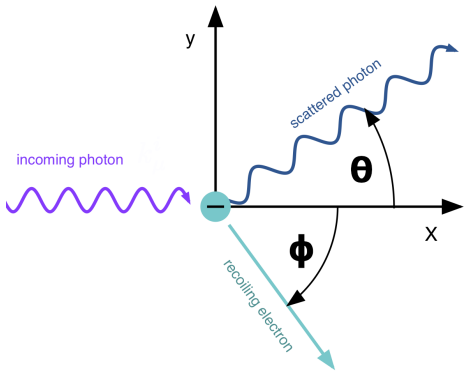

FIG. 1: A diagram of the Compton scattering interaction [7]. A photon is scattered off an electron with a transfer of energy.

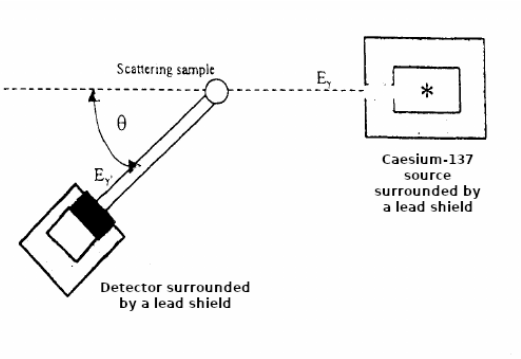

FIG. 2: A schematic of the apparatus used [1].

measured in $\mathrm{cm}^2/\mathrm{sr}$ where r_0 is the classical electron radius, $\alpha = \frac{E_\gamma}{m_0 c^2}$, and $d\Omega$ is the solid angle in steradians. The differential cross-section can also be represented in the measurable quantities in this experiment:

$$\frac{\partial\sigma}{\partial\Omega} = \frac{\Sigma_{\gamma'}}{N\Delta\Omega I} \tag{7}$$

where $\Sigma_{\gamma'}$ is the sum under the photopeak divided by the counting time and the intrinsic peak efficiency, N is the number of electrons in the scattering sample, $\Delta\Omega$ is the solid angle of the detector, and I is the number of incident gamma rays per unit area per second at the scattering sample.

Therefore, in this experiment we will measure the energy of the scattered gamma ray for many different scattering angles and scatter the inverse of the energy against $(1-\cos\theta)$. Using a linear least squares fit to these points we can directly compare the result against the theoretical linear result in equation 5. We will also use the net counts for each angle to determine the differential cross-section and compare it to the Klein-Nishina formula, eq 6.

B. Methodology

1. Apparatus

The apparatus was set up as shown in figure 2. A thallium-activated sodium iodide detector (NaI(Tl)) and a photomultiplier tube were used to detect the gamma rays. This detector was placed inside of a lead shielding which was on rails free to rotate 100 degrees either side of the axis of the emitter and the scattering sample. Electrons in the detector crystal are excited by the gamma rays and the scintillations produced from the return to ground state are detected and produced as signals by a photomultiplier tube. The electronics were turned on prior to taking measurements to allow them to approach working temperature.

A source of Caesium-137 was used as the gamma ray emitter. This source was encased in lead shielding with a closable opening on the side facing towards the detector and scattering sample. A cylinder of aluminium was chosen to be the scattering sample.

2. Calibration

MAESTRO Multichannel Analyser Emulation Software was used to analyse the energy spectrum. Before measurements could be made using the apparatus, the software had to be calibrated to determine the energy at each channel. To do this, two small calibration sources with known gamma ray energy were placed directly in front of the detector so that the rays would arrive directly (no scattering). The two calibration substances used were Caesium-137 and Americium-241, with gamma ray energies of 662 keV and 59.5 keV respectively. Using more calibration sources would increase the accuracy of the calibration, however for the purposes of this experiment, the reduction in uncertainty because of this would be insignificant compared to other uncertainties due to the Gaussian nature of the photopeak and the uncertainty on the angle.

3. Data Collection

Starting from perpendicular to the axis of emission, data were taken in 5 degree steps between 90 and 20 degrees from the emission axis. Angles lower than 20 degrees were not usable as some gamma rays would arrive at the detector unscattered and hence interfere with the analysis. The angles were measured by taking the left and right side of the detector mount on the graduated rail and determining the midpoint. The uncertainty on this measurement was determined to be 0.25 degrees based on half the resolution of the graduation however, as there existed some imprecision

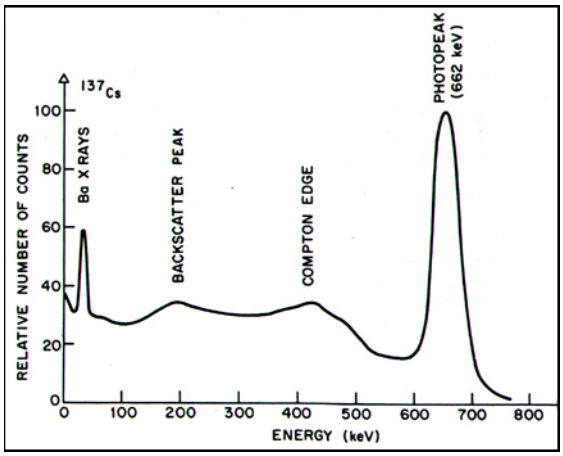

FIG. 3: The spectrum observed from a typical Caesium-137 source [8].

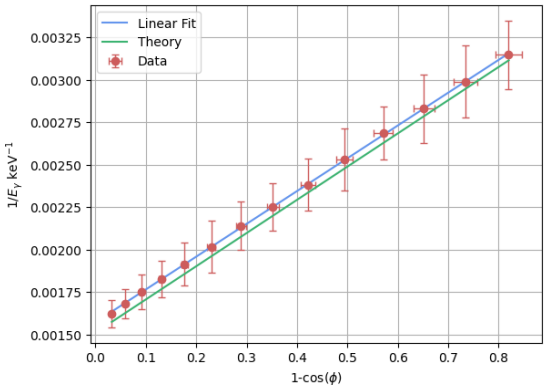

FIG. 4: A scatter plot of the data with a fitted line. This is compared to the theory of equation 5.

in the positioning of the detector in its housing, a more lenient approximation of the uncertainty on the angle of 2 degrees was taken.

The spectrum recorded is similar to that shown in figure 3. Measurements of the photopeak Gaussian were taken from the minimum point between the Compton edge and the photopeak to the end of the high energy tail of the Gaussian of the photopeak. To calculate the net counts, the software assumes a linear transition between this minimum and this gaussian tail to account for multiple scattering occurrences. The angle, photopeak energy, photopeak FWHM, net counts (including uncertainty) and the live time were all recorded in appendix A.

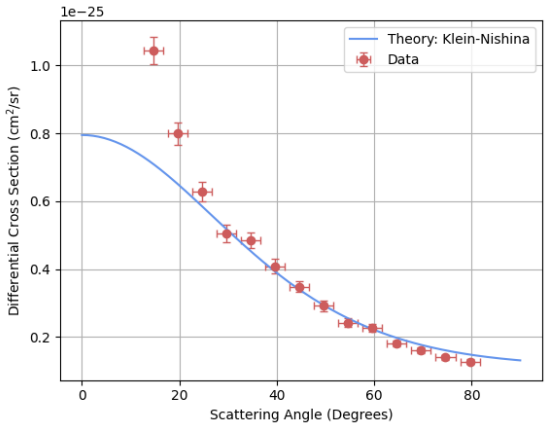

FIG. 5: A scatter plot of the data comparing the measured cross-section to the theoretical values calculated by the Klein-Nishina equation, equation 6.

C. Results and Analysis

The reciprocal of the energy of the scattered gamma ray was plotted against the angle in figure 4. A linear least squares fit was applied and compared to the theory. Note that as the data contained both an uncertainty in the x and y directions an orthogonal distance regression would in theory be a more accurate fit, however as the x uncertainties were mostly insignificant compared to the y uncertanties, for simplicity a least squares fitting was used instead. We see a slight offset from the from the theory line in figure 4 however the slope is very similar. This is likely due to a systematic error in the alignment of the apparatus such as a misalignment of the placement of the detector in its housing. The total uncertainties for this plot were determined by propagating the error on the measured values through their respective equations.

The total net counts under the photopeak were divided by the counting time and plotted against the scattering angle in figure 5, and compared to the Klein-Nishina formula. We see that, as predicted, that the low angle data points deviate from the theory. This is due to the unwanted inclusion of direct gamma rays arriving at the detector unscattered. The data in this plot was initially much lower than the theory values (however still of the same order). The data was multiplied by a constant scalar of 4.95 to match the theoretical line. This was determined visually. This constant offset is likely due to an inaccurate assumption of the activity of the source included in the calculations. The source used is old and would have decayed multiple half-lives since the measurement was taken. Again the total uncertainties for this plot were determined by propagating the error on the measured values through their respective equations.

III. RELATIVITY AND THE ELECTRON REST MASS

A. Theory

In the previous section we assumed that the electrons involved in the scattering process needed to be treated relativistically. We know this must be true as our data follows closely that of the theory, however, this can be tested more rigorously by determining the rest mass of the electron. This can be done by comparing the kinetic energy of the electron and the energy of the scattered gamma ray.

1. Classical Calculation

Similarly to section II.A we must consdier the conservation of energy and momentum in the collision. We know the classical relation between the energy and momentum of a photon to be $E_\gamma = p_\gamma c$. The Compton edge of the gamma ray energy spectrum in figure 3 represents the incident gamma ray being backscattered, i.e. a scattering angle of 180 degrees. Hence by conservation of momentum we have [9]:

$$p_\gamma = p - p'_\gamma \tag{8}$$

where p_γ, p, and p'_γ are the momenta of the incident gamma ray, the electron after scattering, and the scattered gamma ray respectively. By conservation of energy we have:

$$p_\gamma c = p'_\gamma c + T \tag{9}$$

where T is the kinetic energy of the electron. These two equations can be combined to yield an expression for the total energy in terms of the measurable quantities.

$$pc = 2E_\gamma - T \tag{10}$$

In the classical approach, we take the non-relativistic kinetic energy, $T = p^2/2m_{nr}$, were the mass subscript corresponds to the non-relativistic mass. Hence we can substitute the momentum into this expression to find the rest mass of the electron in terms of the measurable quantities.

$$m_{nr} = \frac{p^2c^2}{2T} = \frac{(2E_\gamma - T)^2}{2T} \tag{11}$$

2. Relativistic Calculation

Factoring for special relativity we have the total electron energy equalling the rest mass energy and the kinetic energy,

$$p^2c^2 + (m_0c^2)^2 = (T + m_0c^2)^2 = E_e^2 \tag{12}$$

yielding the energy-momentum relationship for special relativity [9]. We can then relate the rest mass in terms of the measurable quantities:

$$m_0c^2 = \frac{p^2c^2 - T^2}{2T} = \frac{2E_\gamma(E_\gamma - T)}{T} \tag{13}$$

Therefore, by plotting the equations for the classical rest mass and the relativistic rest mass (equations 11 and 13 respectively) and comparing the two, we can see whether the electrons in this reaction need to be treated relativistically.

B. Methodology

Apparatus differences, what sources were used, general procedure

In this experiment a germanium detector was used to measure with high precision.

C. Results and Analysis

Determining the uncertainty based on the channel width of the photopeak.

IV. CONCLUSION

[1] *Compton Scattering Experiment*, UCD School of Physics.

[2] R. Kuroda, H. Toyokawa, M. Yasumoto, H. Ikeura-Sekiguchi, M. Koike, K. Yamada, T. Yanagida, T. Nakajyo, F. Sakai, and K. Mori, Quasi-monochromatic hard x-ray source via laser compton scattering and its application, Nuclear Instruments and Methods in Physics Research Section A: Accelerators, Spectrometers, Detectors and Associated Equipment **637**, S183 (2011), the International Workshop on Ultra-short Electron and Photon Beams: Techniques and Applications.

[3] G. Harding, Inelastic photon scattering: Effects and applications in biomedical science and industry, Radiation Physics and Chemistry **50**, 91 (1997), inelastic Scattering of X-Rays and Gamma Rays.

[4] A. Tortosa, *Comptonization mechanisms in hot coronae in AGN. The NuSTAR view.*, Ph.D. thesis, Universita Degli Studi, Roma TRE (2018).

[5] M. Fowler, The Differential Cross Section, Libre Texts Physics, visited on 03/03/23.

[6] Y. YAZAKI, How the klein–nishina formula was derived: Based on the sangokan nishina source materials, Proceedings of the Japan Academy. Series B. Physical and biological sciences **93**, 399 (2017).

[7] W. Boeglin, Compton scattering, Florida International University, `https://wanda.fiu.edu/boeglinw/courses/Modern_lab_manual3/Compton_Scattering.html`, visited on 02/03/23.

[8] The Analysis Pulse-Height Spectrometry, Virginia Commonwealth University, `http://www.people.vcu.edu/~mhcrosthwait/clrs322/Pulseanalysis.htm`, visited on 03/03/23.

[9] P. L. Jolivette and N. Rouze, Compton scattering, the electron mass, and relativity: A laboratory experiment, American journal of physics **62**, 266 (1994).

Appendix A: Caesium-137 Spectrum Data

Angle Left	Angle Right	Avg Angle	Energy (keV)	FWHM (keV)	Net Counts	Uncertainty	Live Time	Real Time
85	74.25	79.625	317.83	40.64	15837	544	291.22	291.78
80	69.25	74.625	334.51	47.58	13190	492	233.34	233.8
75	64.25	69.625	353.52	50.79	10691	422	175	175.38
70	59.25	64.625	372.42	42.93	10268	389	159.62	160
65	54.25	59.625	395.22	56.93	11211	365	148.16	148.56
60	49.25	54.625	419.84	53.42	10695	424	142.16	142.56
55	44.25	49.625	444.27	55.75	10546	413	123.58	125.86
50	39.25	44.625	467.43	62.32	16675	502	173.28	176.08
45	34.25	39.625	496.4	75.68	13302	403	126.08	128.92
40	29.25	34.625	522.44	69.37	10987	332	92.9	95.28
35	24.25	29.625	547.42	64.57	11012	453	94.36	96.98
30	19.25	24.625	571.76	66.64	14872	457	107.78	109.78
25	14.25	19.625	594.79	61.57	15089	440	89.82	92.68
20	9.25	14.625	616.41	61.76	17480	459	82.9	85.18